Rearrangement and Fragmentation Processes on the Potential Energy Surfaces of the $(CH_nS)^+$ ($n = 1-4$) Systems

Raman Sumathi and S. D. Peyerimhoff*

Lehrstuhl fur Theoretische Chemie, Universitat Bonn, Wegelerstrasse 12 D-53115 Bonn, Germany

Debasis Sengupta

Department of Chemical, Bio and Materials Engineering, Arizona State University, Box 876006, Tempe, Arizona 85287-6006

Received: September 10, 1998; In Final Form: December 1, 1998

Stationary points on the quartet and doublet surfaces of $(CH_4S)^+$, on the triplet and singlet surfaces of $(CH_3S)^+$, on the doublet surface of $(CH_2S)^+$, and on the singlet and triplet surfaces of $(CHS)^+$ have been examined by ab initio molecular orbital theory. Equilibrium and saddle point geometries have been located at second-order perturbation theory (UMP2) level using a 6-311++G(d,p) basis set. Relative energies were obtained by means of extensive quadratic configuration interaction singles and doubles calculations with a 6-311++G(2df,2pd) basis set. On the quartet $(CH_4S)^+$ surface, an association complex stabilized by 25.2 kcal/mol with respect to CH_4 and $S^+(^4S)$ has been identified. Owing to its large barrier (55.5 kcal/mol) for its dissociation, it is expected to be long-lived as assumed by Zakouril et al. (*J. Phys. Chem.* **1995**, *99*, 15890) in their experimental work. On the $(CH_4S)^+$ doublet surface, the conventional methanethiol radical cation (CH_3SH^+) is more stable than the ylide ion $(CH_2SH_2^+)$ and depending upon the entrance channel, one can expect a competitive isomerization and dissociation. Cleavage of the C−H bonds in the ylide ion involves higher barriers compared to that in CH_3SH^+. Three stable isomers, viz., CH_3S^+, CH_2SH^+, and $CHSH_2^+$, have been located on the singlet and triplet surfaces of the $(CH_3S)^+$ system. While CH_2SH^+ is more stable on the singlet surface, CH_3S^+ is more stable on the triplet surface. The molecular hydrogen elimination requires higher barriers from all these isomers compared to radical dissociation. CH_2S^+ is predicted to be more stable than *trans*-$HCSH^+$ with a barrier of 51.9 kcal/mol for the rearrangement to the less stable isomer. A significant barrier to 1,2 hydrogen shift isomerization is predicted on the triplet surface of the HSC^+ while that on the singlet surface is predicted to occur without activation energy. The latter signifies an unstable HSC^+ minimum on the singlet surface.

1. Introduction

Studies of ion−molecule reactions of the sulfur ion S^+ are mostly motivated by the importance of these reactions in interstellar clouds.[1−3] Experimental research on reactions of the S^+ ion has been carried out in ICR experiments,[4−6] flowing afterglows,[7,8] flow drift tube experiments,[9] and selected ion flow tube (SIFT) experiments.[1,10,11] Recently, by using the selected ion flow drift tube (SIFDT) technique, Zakouril et al.[12] have investigated a number of fast ion−molecule reactions, the reaction rate coefficients of which decrease strongly when KE_{CM} (the reactant ion/reactant molecule average center-of-mass collision energy) increases from thermal values up to a few electronvolts. They measured the reaction rate coefficients and the product distributions for the reactions of ground-state $S^+(^4S)$ with small hydrocarbon molecules CH_4, C_2H_2, C_2H_4, and C_3H_8 as a function of KE_{CM} and observed pronounced negative energy dependencies of the rate constant. This suggests that these reactions proceed via the formation of long-lived complexes. In the early ICR experiments,[4] the product SCH_3^+ was observed and the measured reaction rate coefficient was 1.4×10^{-10} cm^3 s^{-1}. In the SIFT study of Tichy et al.[11] thermal reaction rate coefficients of the ground state $S^+(^4S)$ and excited states $S^+(^2D)$ and $S^+(^2P)$ with CH_4 have been determined. The measured values are 3.5×10^{-10} and 1.3×10^{-9} cm^3 s^{-1} for the sulfur ion in its ground and excited states, respectively. Only SCH_3^+ ion has been reported as a product for the reaction of the ground state S^+ ion.

Though the structure, thermochemistry, and reactivity of some sulfur-bearing ions with neutral molecules have been the subject of theoretical studies,[13,14] the reaction of S^+ in its quartet multiplicity with methane has not yet been investigated theoretically. Although a number of experimental studies have provided evidence as to the structures and stabilities of the possible isomers of CH_3S^+,[15] thioformaldehyde cation (CH_2S^+), the thiohydroxycarbene cation $(HCSH^+)$, the thioformyl cation (HCS^+), and the isomer HSC^+,[16] a rigorous theoretical study involving all isomers and their dissociation/isomerization channels at a reasonably high level of calculation is still not available for the kinetic characterization of the reactions of S^+.

The purpose of the present work is, therefore, to explore theoretically those features of the potential energy surfaces (PES) of $(CH_4S)^+$ (doublet and quartet surfaces), $(CH_3S)^+$ (triplet and singlet), $(CH_2S)^+$ (doublet), and $(CHS)^+$ (triplet and singlet) cations which are expected to be of potential significance in understanding their dissociation dynamics. These features are

* Corresponding author. Fax: 49-228-739064. E-mail: unt000@IBM.rhrz.uni-bonn.de.

10.1021/jp983656b CCC: $18.00
Published on Web 01/22/1999

SCHEME 1

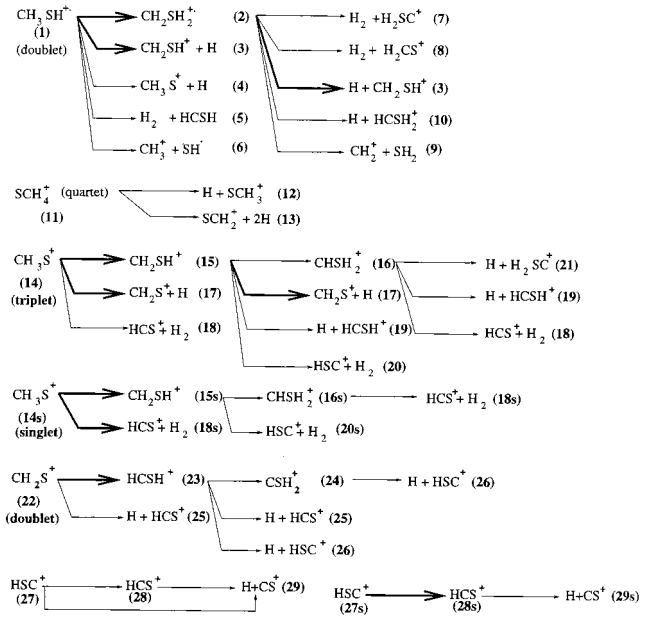

qualitatively sketched in Scheme 1 and may be summarized as follows.

(a) The structure and relative energetics of the various isomers of $(CH_4S)^+$ in its quartet and doublet states, $(CH_3S)^+$ in its singlet and triplet states, $(CH_2S)^+$ in its doublet state and $(CHS)^+$ in its singlet and triplet states.

(b) The transition states for the isomerization, dissociation, and elimination reactions of SCH_n^+ into $H + SCH_{n-1}^+$, and $H_2 + SCH_{n-2}^+$, respectively.

Previous experimental and theoretical studies on SCH_n^+ ($n = 1-4$) are reviewed in section 3, while the computational details and results of the present investigations are summarized and discussed in sections 4 and 5 under different subtopics.

2. Experimental and Theoretical Background

The equilibrium structure of the ylide ions or the distonic radical cations, $^{\bullet}CH_2X^+H$, and its conventional isomers $CH_3X^{\bullet+}$ ($X = F$, OH, NH_2, Cl, SH, and PH_2) have been computationally determined by Radom et al.[17] at the perturbation level with a large basis set, MP2/6-311+G(2df,p), to improve the previous knowledge on the structures and thermochemical properties of these species. Their results demonstrate that a fairly satisfactory description of structures is provided by MP2/6-311++G(d,p) computations and that zero-point vibrational energies can be obtained fairly reliably by appropriately scaled MP2/6-311++G(d,p) harmonic vibrational frequencies. Also optimization at MP2/6-311++G(d,p) level is shown[18] to give comparable geometries with the state-of-art CCSD(T)/6-311++G(d,p) method for the H-loss transition structures in radicals and radical cations. The former has a general tendency to decrease the dissociating X−H ($X = P$, N, O, S, and C) bond length by a maximum of 0.1 Å. For this reason, we choose the same level of theory for the full characterization of the various PES's of $(CH_nS)^+$ ($n = 1-4$) ions. The experimental investigations[19] and most of the theoretical studies[17,20] on CH_4S^+ are restricted largely to thermochemical data. Radom et al.,[20c,d] in their earlier investigation on the doublet potential energy surface of the CH_4S^+ system at the MP3/6-31G**//6-31G* level, have identified transition states for three reaction channels viz., $CH_3SH^+ \rightarrow CH_2SH_2^+$, $CH_3SH^+ \rightarrow CH_2SH^+ + H^{\bullet}$, and $CH_2SH_2^+ \rightarrow CH_2SH^+ + H^{\bullet}$. All these pathways are marked with bold arrows in Scheme 1. They confirmed that the ylide ions are more stable with respect to unimolecular rearrangement or decomposition than their neutral counterparts.

The $(CH_3S)^+$ system has been the subject of several theoretical studies in a different context.[20c,21-23] Most of these deal with the thermochemistry and proton affinity of these molecular ions. Collisional activation mass spectra[15] suggest the protonated thioformaldehyde, $H_2C{=}SH^+$ to be more stable compared to the thiomethoxy CH_3S^+ structure. Flores et al.[24] have studied the reaction of CH_3^+ with the ground state sulfur atom (^3P) at MP2/6-31G** level and they concluded that the channel giving rise to $SCH_2^+(^2B_2) + H(^2S)$ is the preferred one. The reaction pathways investigated by them are shown in bold arrows in Scheme 1. Some of the stationary points (as shown in Scheme 1 with bold arrows) on the doublet potential energy surface of the thioformaldehyde cation, $(CH_2S)^+$, have been examined by Pope et al.[25] at the SCF level. $CH_2S^+(^2B_2)$ was predicted to be more stable than *trans*-$HCSH^+$ and the 1,2 hydrogen shift isomerization is predicted to occur without any barrier.

Thus, rigorous ab initio calculations on $(CH_nS)^+$ ($n = 1-4$) systems at a consistent level of characterization are still lacking. We are unaware of any previous studies on the $(CH_4S)^+$ quartet surface, or the stability of the various isomers. Furthermore, no previous attention appears to have been given to the molecular elimination of H_2 from $(CH_nS)^+$ ($n = 1-4$). Moreover, the PES's have not been analyzed in the perspective of the kinetics of the reaction between S^+ and CH_n species. Our goal is, therefore, to calculate optimum PESs of all possible pathways originating in the reactions of S^+ and CH_4 in order to obtain a complete picture of the reaction mechanism.

3. Computational Details

Ab initio molecular orbital calculations were carried out using the Gaussian 94 set of programs.[26] The open-shell calculations were performed using the unrestricted Hartree−Fock formalism. As a measure of the UHF spin contamination, we note that the expectation value of $\langle S^2 \rangle$ operator was not greater than 0.765 for doublets, 2.19 for triplets, and 3.752 for quartets. The potential energy surface was initially mapped out using SCF calculations in conjunction with the 6-31G(d,p) basis set. The identity of each first-order stationary point is determined when necessary, by intrinsic reaction coordinate (IRC) calculations. Geometries of the relevant equilibrium and transition structures were then reoptimized using the MP2/6-311++G(d,p) basis set. All electrons were considered for correlation correction. Computed energies of all stationary points were further improved by single-point QCISD(T) calculations at the MP2 geometries with the larger 6-311++G(2df,2pd) one-electron basis set. The zero-point energies were derived from harmonic vibrational wavenumbers at the UMP2/6-311++G(d,p) level and scaled down by a uniform factor of 0.94. Throughout this paper, bond lengths are given in angströms, bond angles in degrees, and zero-point and relative energies in kcal/mol, unless otherwise stated.

4. Results and Discussion

The reactions investigated in the present study are listed in Scheme 1. The QCISD(T)/6-311++G(2df,2pd)//MP2/6-311++G(d,p) relative energies with appropriate zero-point vibrational energy corrections are shown in Figure 1a−d. Let us first describe briefly the essential features of the lowest-lying doublet and quartet PES's related to the $(CH_4S)^+$ system (see Figure 1a). Each stationary point in Figure 1 is labeled with a number in order to facilitate the discussion. While the minima

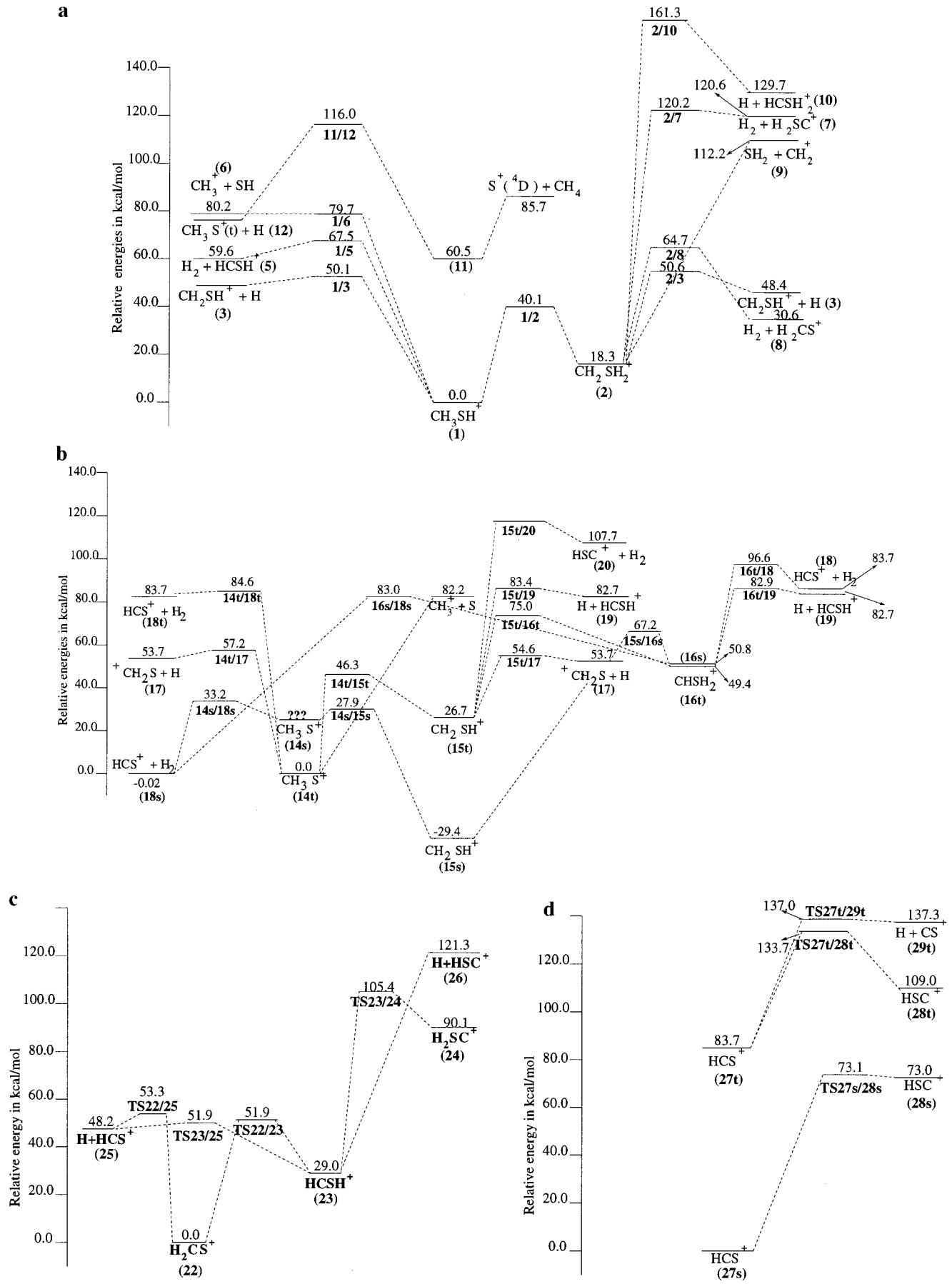

Figure 1. Overall profile of (a) doublet and quartet PES for the $(CH_4S)^+$, (b) singlet and triplet PES for the $(CH_3S)^+$, (c) doublet PES for the $(CH_2S)^+$, and (d) singlet and triplet PES for the $(CHS)^+$ systems calculated at QCISD(T)/6-311++G(2df,2pd)//MP2/6-311++G(d,p)+ZPE level of theory.

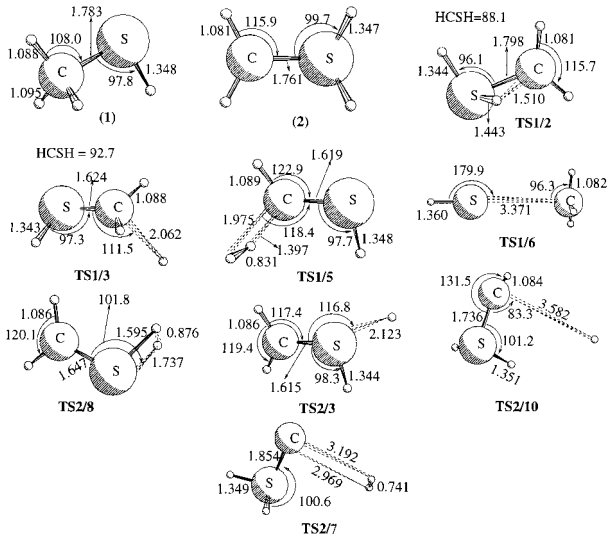

Figure 2. MP2/6-311++G(d,p) optimized geometries of the stationary points on the doublet $(CH_4S)^+$ energy surface.

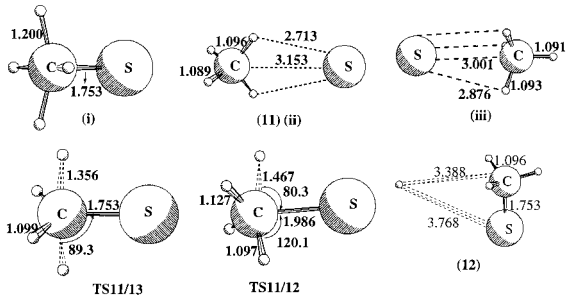

Figure 3. MP2/6-311++G(d,p) optimized geometries of the stationary points on the quartet $(CH_4S)^+$ energy surface.

on the various electronic surfaces of $(CH_nS)^+$ ($n = 1-4$) are associated with the numbers from **1** to **28**, the transition structures (TS) connecting two minima **X** and **Y** are defined by **X**/**Y**.

The doublet PES of $(SCH_4)^+$ consists of two isomers, namely CH_3SH^+ (**1**) and $CH_2SH_2^+$ (**2**) and the different first-order saddle points connecting these minima to different product limits viz., $CH_2SH^+ + H$ (**3**), $CH_3S^+ + H$ (**4**), $H_2 + HCSH^+$ (**5**), $CH_3^+ + SH$ (**6**), $H_2 + H_2SC^+$ (**7**), $H_2 + H_2CS^+$ (**8**), $CH_2^+ + SH_2$ (**9**), and $H + HCSH_2^+$ (**10**). The MP2/6-311++G(d,p) optimized geometries of the transition states **1**/**2**, **1**/**3**, **1**/**5**, **1**/**6**, **2**/**7**, **2**/**8**, **2**/**9**, and **2**/**10** on the doublet potential energy surface are shown in Figure 2, while the stationary points on the quartet PES viz., **11**, **11**/**12**, and **11**/**13** are shown in Figure 3.

The optimized structures of the three isomers of $(CH_3S)^+$ ((**14**), (**15**), and (**16**)) in their ground state and the transition structures on the lowest lying triplet $(CH_3S)^+$ PES are given in Figure 4 while those on the singlet surface are shown in Figure 5. The optimized structures of the three isomers of $(CH_2S)^+$ (**22**, **23**, and **24**) and the saddle point geometries on its doublet PES are presented in Figure 6 along with the structures of the stationary points on the $(CHS)^+$ PES. The unscaled harmonic vibrational frequencies of the various stationary points on the $(CH_nS)^+$ ($n = 4-1$) are available as Supporting Information as they are of interest to the modeling kineticists for the estimation of the rate constants.

4.1. Doublet and Quartet PES's of the $(CH_4S)^+$ System. The QCISD(T)/6-311++G(2df,2pd)//MP2/6-311++G(d,p) energies are shown in Figure 1a relative to that of the doublet CH_3SH^+ minimum (**1**) with appropriate zero-point vibrational

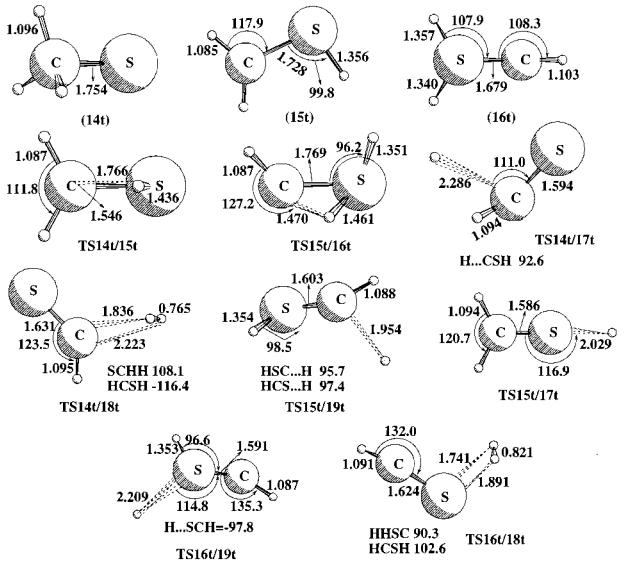

Figure 4. MP2/6-311++G(d,p) optimized geometries of the stationary points on the triplet $(CH_3S)^+$ energy surface.

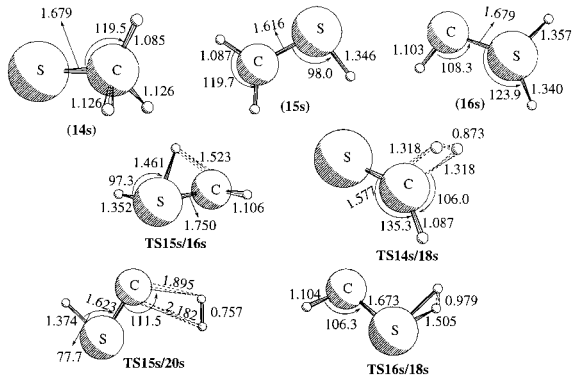

Figure 5. MP2/6-311++G(d,p) optimized geometries of the stationary points on the singlet $(CH_3S)^+$ energy surface.

energy corrections using the UMP2 frequencies. The most important result is perhaps the fact that both the doublet and quartet PES's are well separated from each other. As observed by Radom et al.,[20] on the doublet PES, the conventional isomer CH_3SH^+ (**1**) was found to be energetically more stable than the ylide ion (**2**) by 21.9 kcal/mol. The ylide ion has two C_s structures which are energetically close to each other (0.2 kJ mol^{-1}) with the anti conformation being more favored over the syn. $CH_2SH_2^+$ has a C−S bond length of 1.761 Å, which is shorter than that in CH_3SH^+ (1.783 Å).

It is readily seen in Figure 1 that all processes involving isomerization and radical and molecular dissociations from CH_3SH^+ (**1**) are endothermic and involve appreciable barriers. We therefore expect a relatively long lifetime and a possibility to isolate the isomeric species of $(CH_4S)^+$ system experimentally. The 1,2-hydrogen shifts from the carbon to the sulfur and the reverse occur from the anti (C_s) isomer with the latter being energetically favored over the former migration. The calculated three-membered TS **1**/**2** for this shift has hydrogens being perpendicular to each other on carbon and sulfur. In addition to this 1,2-hydrogen shift, **1** can undergo the hydrogen radical dissociation via the cleavage of either the C−H (**1**/**3**) or the S−H bond and the molecular elimination of H_2 (**1**/**5**). The stretching of the S−H bond leads to the direct dissociation limit ($CH_3S^+(s) + H$) and hence it does not proceed via a specific transition state. The 1,1-elimination of H_2 requires an appreciable barrier and is therefore less favored compared to the isomer-

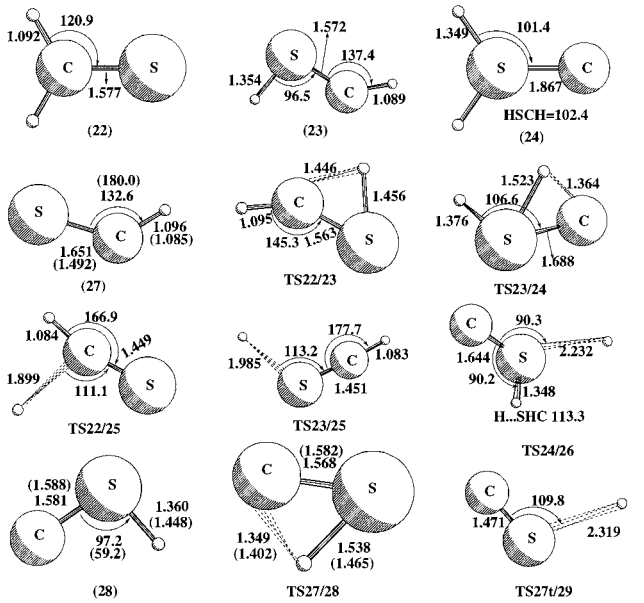

Figure 6. MP2/6-311++G(d,p) optimized geometries of the stationary points on the doublet $(CH_2S)^+$ and singlet and triplet $(HCS)^+$ energy surfaces. Numbers in parentheses correspond to the singlet state geometries.

ization to ylide ion. Consequently, the most favorable channel for the disappearance of CH_3SH^+ seems to be the isomerization to the ylide ion, $CH_2SH_2^+$.

The ylide ion **2** once thus formed can undergo molecular elimination of H_2 to form either the thioformaldehyde cation, H_2CS^+, or the isomeric H_2SC^+. It can also dissociate yielding $H + HCSH_2^+$ and $H + HSCH_2^+$ cations. All these processes have been investigated and the saddle points have been identified (Figure 2). Cleavage of a H or the 1,1 elimination of H_2 from the carbon of the $CH_2SH_2^+$ cation proceeds via high-energy transition states (**TS2/10**, **TS2/7**) and hence are expected not to play a major role in the ylide ion disappearance. Both processes are highly endothermic and the transition structures are productlike. As can be seen from Figure 1a, the formation of both $H + CH_2SH^+$ (**3**) and $H_2 + H_2CS^+$ (**8**) involves lower barriers in comparison to other dissociation channels. However, these barriers are 10.5 and 24.6 kcal/mol, respectively, higher than the barrier for isomerization to $CH_3SH^\bullet$. Since the rate-determining step is not the isomerization process, the formation of **3** is possible both via isomerization of **2** and directly from **2**. Similarly, **3** can be formed from **1** via its isomerization to **2** and also via direct dissociation. It should be pointed out that the positions of the transition structures **1**/**3** and **2**/**3** are very close to each other in the energy scale.

The cleavage of the C−S bond in both CH_3SH^+ and $CH_2SH_2^+$ ions was calculated to be a direct destabilization process. The ground state potential energy curves are monotonically destabilized. The reactions are endothermic and the dissociation limits are achieved at a very large C−S distance. This, in turn, suggests a possible mode of generation of $(CH_4S)^+$ species (barrierless recombination). The species thus generated from CH_3^+ and SH (or CH_2^+ and SH_2) will be an energized molecule and can undergo fast isomerization and various dissociation reactions which are otherwise difficult by thermal activation of $(CH_4S)^+$. Under these conditions, high pressures are needed for the isolation of CH_3SH^+ and $CH_2SH_2^+$ ions. Nevertheless, the doublet PES clearly establishes the long lifetime of the isomers of $(CH_4S)^+$ at ordinary temperatures.

On the quartet surface, three different structures, as shown in Figure 3, have been obtained. The structure (i) with a pentacoordinated carbon involving a C−S bond (1.753 Å) is found to be a saddle point with respect to CH_2 bending vibrations with an imaginary frequency of 1789i cm^{-1}. It has a distorted trigonal bipyramidal structure and all the hydrogens make an angle of 104.1° with the sulfur atom (∠HCS). All our attempts to find a regular trigonal bipyramidal geometry have proven futile. The structure (ii) wherein the sulfur atom is along the C_2 axis of CH_4 is found to be a minimum. It is an association complex between S^+ and methane and is stabilized by 25.2 kcal/mol. The C−H bonds in methane are polarized as $C(\delta^-)-H(\delta^+)$. The structure (iii) with a tricoordinated S^+ is also found to be a minimum and has approximately the same energy as (ii) ($\Delta E = 0.5$ kcal). We could not locate stable structures corresponding to the ylide ion ($CH_2SH_2^+$) or its (CH_3SH^+) isomer on the quartet PES.

Two different reaction channels, viz., $CH_4S^+ \rightarrow CH_3S^+ + H^\bullet$ (**12**) and $CH_4S^+ \rightarrow CH_2S^+ + 2H^\bullet$, have been investigated and the corresponding saddle points are shown in Figure 3. The pathway for the hydrogen radical dissociation is summarized in Table 1. These data were obtained by following the IRC calculation from **11**/**12** back to the reactant and forward to the products. The data presented here were determined at the MP2/6-311++G(d,p) level to present a more accurate picture of the geometric changes. Minima were found on both sides of the reaction coordinate and they are shown in Figure 3. As shown in Table 1, the dominant changes as the molecule proceeds from the reactant to its product are represented by a shortening of the C−S bond in conjunction with an increase in one of the C−H bond lengths. Also the angle made by the detaching hydrogen with S widens up with a simultaneous narrowing down of other HCS angles.

As is obvious from Figure 1a, the association complex CH_4S^+ formed from the reaction of $S^+(^4S) + CH_4$ can either dissociate back to the reactants or to $CH_3S^+ + H$ products. Since the barrier for the product formation is higher than that for redissociation, at low KE_{CM}, the complex is expected to be long-lived and the reaction rate coefficient should correspond to the capture rate coefficient. Increasing the KE_{CM} at low KE_{CM} would tend to increase the redissociation rate coefficient and hence would have a negative energy dependence. However, when the energy is above the saddle point, **TS11/12**, energy, further increase in energy will increase the rate coefficient for product formation and hence the total rate coefficient will have a positive energy dependence. This qualitatively explains the experimental observations of Zakouril et al.[12]

4.2. Singlet and Triplet PES's of $(CH_3S)^+$ System. The low-lying isomer of the $(CH_3S)^+$ system is a $^1A_1$ state of the mercaptomethyl cation (**15s**) and it has been examined in several previous theoretical studies.[20−24] The singlet state of CH_2SH^+ has a significantly shorter C−S bond length (1.616 Å) than that in the triplet state (1.761 Å). The $^3A''-^1A'$ energy difference equals 56.1 kcal/mol. In contrast to the earlier investigation,[21] we could not locate a minimum on the singlet potential energy surface of thiomethoxy cation **14s**. The optimized structure shown in Figure 4 has an imaginary frequency of 605i cm^{-1} and lies energetically 28.3 kcal/mol above (**14t**). The other carbene isomer of $(CH_3S)^+$, viz., $HCSH_2^+$ (**16**), is approximately 50 kcal/mol above **14t** and involves appreciable barrier for its formation from CH_2SH^+ on both the triplet (48.3 kcal/mol) and singlet (96.6 kcal/mol) potential surfaces. On the singlet surface, these isomers can undergo H_2 elimination besides isomerization to the other isomers. However, as can be seen from Figure 1b, the barrier heights for the elimination of H_2 are higher than the

TABLE 1: Results of MP2/6-311++G(d,p) Calculations for the Intrinsic Reaction Coordinate of $SCH_4^+ \rightarrow H^\bullet + SCH_3^+$

reaction coordinate	rel energy	R_{C-S} Å	$R_{C\cdots H}$ Å	R_{C-H2} Å	R_{C-H4} Å	∠SCH1	∠SCH2	∠SCH3	H2CSH1	H4CSH1
−2.69	−68.9	3.193	1.095	1.089	1.095	56.937	124.7	56.4	90.2	180.2
−2.39	−68.8	3.036	1.096	1.089	1.095	56.458	124.7	57.7	89.5	180.0
−2.09	−68.2	2.878	1.096	1.090	1.095	56.508	124.6	58.8	88.9	180.0
−1.79	−66.6	2.720	1.096	1.091	1.095	56.525	124.5	60.6	88.1	180.0
−1.49	−63.3	2.564	1.096	1.093	1.093	57.493	124.8	62.7	86.9	180.0
−1.19	−57.3	2.416	1.113	1.097	1.092	60.548	125.3	66.1	85.2	180.0
−0.89	−46.4	2.289	1.174	1.100	1.096	65.452	125.3	70.8	83.3	180.0
−0.29	−9.8	2.082	1.363	1.099	1.116	76.020	122.6	80.6	79.9	180.0
0.00	0.0	1.986	1.466	1.097	1.126	80.352	120.0	85.2	78.0	180.0
0.29	−5.9	1.892	1.576	1.094	1.131	83.640	117.5	89.4	75.9	180.0
0.89	−23.2	1.768	1.833	1.091	1.122	88.015	114.2	97.9	69.9	180.0
1.19	−29.4	1.753	1.979	1.092	1.112	89.160	112.7	101.6	66.5	180.0
1.49	−34.1	1.751	2.130	1.092	1.105	89.824	111.2	104.4	63.9	180.0
1.79	−37.4	1.752	2.285	1.093	1.101	90.083	110.1	106.2	62.2	180.0
2.09	−39.6	1.752	2.443	1.094	1.099	90.382	109.5	107.3	61.2	180.0
2.39	−41.1	1.752	2.601	1.094	1.098	90.601	109.1	107.8	60.7	180.0
2.69	−42.1	1.753	2.760	1.095	1.097	90.519	109.0	108.2	60.4	179.9
2.99	−42.6	1.752	2.918	1.095	1.096	90.391	108.8	108.4	60.1	179.9
3.59	−43.2	1.752	3.233	1.096	1.096	89.560	108.7	108.6	59.9	179.8
3.88	−43.3	1.753	3.388	1.096	1.096	88.298	108.7	108.7	59.9	179.9

isomerization barriers. Hence, the singlet mercaptomethyl cation could be long-lived for its isolation.

On the triplet surface, thiomethoxy cation (**14t**) is the most stable isomer and all isomerization and dissociation channels arising from this species are endothermic. A general observation in the $(CH_3S)^+$ PES is that the molecular elimination involves relatively higher barriers compared to the hydrogen radical dissociations. However, the analysis of the reverse ion−molecule reaction, $H_2 + HCS^+ \rightarrow$ products, seems to be more interesting from the perspective of the generation of the H_2CS^+ species which are observed in interstellar clouds. The important criteria for a gas-phase reaction to occur under interstellar conditions is that it is close to barrier-free and exothermic. As can be seen from Figure 1b, the reaction $H_2 + HCS^+$ (**18t**) $\rightarrow H_2CS^+ + H$ is exothermic by 30.0 kcal/mol and the reaction can proceed almost spontaneously except for a very small initial barrier of 0.9 kcal/mol for the formation of CH_3S^+ via the following routes

$$H_2 + HCS^+ (\mathbf{18t}) \xrightarrow{\mathbf{14t/18t}} CH_3S^+ (\mathbf{14t}) \xrightarrow{\mathbf{14t/15t}} CH_2SH^+ (\mathbf{15t}) \xrightarrow{\mathbf{15t/17}} CH_2S^+ + H (\mathbf{17})$$

$$H_2 + HCS^+ (\mathbf{18t}) \xrightarrow{\mathbf{14t/18t}} CH_3S^+ (\mathbf{14t}) \xrightarrow{\mathbf{14t/17}} CH_2S^+ + H (\mathbf{17})$$

Therefore, on the basis of our results, the reaction of H_2 with HCS^+ can be a possible interstellar process.

On the other hand, if the covalently bonded CH_3S^+ is formed from $CH_3^+ + S$ then it will be an energized system with an excess energy of 83.0 kcal/mol and therefore be expected to undergo rapid isomerization to (**15t**) followed by dissociation to $CH_2S^+ + H$. One would also expect a competitive dissociation and isomerization from **14t**. Detailed kinetic analysis will provide the product branching ratios and the contribution of each rate coefficient to the total rate coefficient. Presently calculated more complete PES, vibrational frequencies, and moments of inertia of the various stationary points will be of much use in such kinetic analysis.

4.3. Doublet PES of the $(CH_2S)^+$ Species. The optimized geometries and the relative energies of the various isomers of $(CH_2S)^+$ system viz., $^2B_2$ state of H_2CS^+ (**22**), the trans isomer of the thiohydroxy carbene cation ($HCSH^+$) (**23**) and the carbene (SH_2C^+) (**24**), 1,2-hydrogen shift rearrangement transition states (**TS22/23**, **TS23/24**), and the radical dissociation transition states (**TS22/25**, **TS23/25**) are given in Figures 6 and 1c, respectively. H_2CS^+ is predicted to be more stable than $HCSH^+$ by 29.0 kcal/mol at the QCISD(T)/6-311++G(2df,2pd)//MP2/6-311++G(d,p) level and this is in good agreement with the estimated separation of about 1 eV for the $H_2CS^+/HCSH^+$ in the photoionization mass spectrometric measurements.[16] While considering the reaction of $H + HCS^+$, the incoming hydrogen can attack either at the carbon or at the sulfur end of the thioformyl cation. The barrier for the hydrogen attack at the C center of HCS^+ ($H + HCS^+$ (**25**) $\rightarrow H_2CS^+$ (**22**)) was calculated to be 5.1 kcal/mol. However, the attack at the S end ($H + HCS^+ \rightarrow$ *trans*-$HCSH^+$) involves a relatively smaller barrier (3.7 kcal/mol). Hence, the $H + HCS^+$ reaction would proceed to a greater extent via **23**. Since the isomerization barrier from $HCSH^+$ is nearly the same as that for dissociation, and because the preexponential factors for dissociation are generally higher than that for isomerization (because the former involves a relatively loose transition state compared to the latter), it would be difficult to isolate the isomers of $(CH_2S)^+$ species in the reactions of $H + HCS^+$. On the other hand, association of H and HSC^+(s) proceeds without any activation barrier to $HCSH^+$ and finally transforms into $H + HCS^+$. Figure 1d shows that the singlet HSC^+ isomerizes to HCS^+ without any barrier while in the triplet state this process has appreciable barrier. Hence, isomerization of singlet HSC^+ is expected to be very fast via both direct and indirect pathways. Of the two dissociation channels from $HCSH^+$, cleavage of the S−H bond is more favored over that of the C−H bond and the latter does not proceed via a specific transition state. As in the case of $(CH_3S)^+$ system, we do not expect any significant role of carbene (**24**) in the unimolecular dissociation dynamics of CH_2S^+ species.

4.4. Singlet and Triplet PES of the $(CHS)^+$ Species. The optimized geometries and the relative energies for the stationary points on the potential energy surface of the thioformyl cation $(HCS)^+$ are given in Figures 6 and 1d, respectively. In agreement with the earlier investigations,[21,16b] the C−S bond in HCS^+ is shorter than in the neutral CS and has increased by 0.13 Å relative to CS in HSC^+. The C−H bond dissociation energy of 137.3 kcal/mol in HCS^+ is in close agreement with the earlier result[25] of 136.6 kcal/mol at the MRDCI+QC level. As can be seen from Figure 1d, HSC^+ is expected to be highly unstable on the singlet surface as there exists almost no barrier for

migration of the H atom from the sulfur to the carbon of the C−S bond. Nevertheless, a minimum characterized by all real vibrational frequencies has been located for HSC^+ with a H−S bond length of 1.448 Å. In contrast, on the triplet surface, appreciable barrier exists for its isomerization to HCS^+ as well as for its dissociation into $H + CS^+$. Hence, the triplet HSC^+ appears to be stable to dissociation and isomerization.

5. Conclusions

The present study provides the first consistent and fairly complete study of the transition-state geometries and barrier heights for the isomerization, radical dissociations, and molecular eliminations of the $(CH_nS)^+$ ($n = 1-4$) systems on various electronic surfaces. The PES's further qualitatively explain the observed reaction kinetics. On the quartet suface of CH_4S^+, a stable association complex of CH_4 and S^+ has been located and is expected to be long-lived owing to its barrier for its dissociation into $CH_3S^+ + H$. Therefore, the rate coefficient of this ion−molecule reaction is primarily limited by the capture rate coefficient of the collision complex. On the doublet surface, the methanethiol cation is more stable compared to the ylide ion. However, it is possible to isolate the ylide ion due to the fact that the barrier for its isomerization is smaller than the barriers for its dissociations starting from either the CH_3SH^+ or the $CH_2SH_2^+$ potential wells.

The relative energy ordering for the $(CH_3S)^+$ system on the triplet surface is $CH_3S^+ < CH_2SH^+ < CHSH_2^+$ while on the singlet surface it is $CH_2SH^+ < CH_3S^+ < CHSH_2^+$. The reaction between molecular hydrogen and thioformyl cation could be an interstellar process leading to the formation of CH_2S^+ ions. Isomerization of HSC^+ to HCS^+ on the singlet surface is spontaneous even in the presence of hydrogen.

Acknowledgment. R.S. thanks Alexander von Humboldt Stiftung for financial support.

Supporting Information Available: Tables of unscaled harmonic vibrational frequencies of various stationary points on $(CH_nS)^+$ ($n = 1-3$). This material is available free of charge via the Internet at http://pub.acs.org.

References and Notes

(1) Smith, D.; Adams, N. G.; Giles, K.; Herbst, E. *Astron. Astrophys.* **1988**, *200*, 191.

(2) Millar, T. J.; Herbst, E. *Astron. Astrophys.* **1990**, *231*, 466.

(3) Smith, D. *Chem. Rev.* **1992**, *92*, 1473.

(4) Huntress, W. T.; Pinizzotto, R. F. *J. Chem. Phys.* **1973**, *59*, 4743.

(5) Laudenslager, J. B.; Huntress, W. T., Jr. *Int. J. Mass Spectrom. Ion Phys.* **1974**, *14*, 435.

(6) Anicich, V. G. *J. Phys. Chem. Ref. Data* **1993**, *22*, 1469.

(7) Fehsenfeld, F. C.; Ferguson, E. E. *J. Geophys. Res.* **1973**, *78*, 1699.

(8) Liddy, J. P.; Freeman, C. G.; McEwans, M. *J. Astrophys. Lett.* **1975**, *16*, 155.

(9) Dotan, I.; Fehsenfeld, F. C.; Albritton, D. L. *J. Chem. Phys.* **1979**, *71*, 4762.

(10) Smith, D.; Adams, N. G.; Lindinger, W. *J. Chem. Phys.* **1981**, *75*, 3365.

(11) Tichy, M.; Rakshit, A. B.; Lister, D. G.; Twiddy, N. D.; Adams, N. G.; Smith, D. *Int. J. Mass Spectrom. Ion Phys.* **1979**, *29*, 231.

(12) Zakouril, P.; Glosik, J.; Skalasky, V.; Lindinger, W. *J. Phys. Chem.* **1995**, *99*, 15890.

(13) Barrientos, C.; Largo, A. J. *J. Phys. Chem.* **1992**, *96*, 5808.

(14) Chiu, S. W.; Li, W. K.; Tzeng, W.; Ng, C. Y. *J. Chem. Phys.* **1992**, *97*, 6557.

(15) Dill, J. D.; McLafferty, F. W. *J. Am. Chem. Soc.* **1979**, *101*, 6526.

(16) Kutina, R. E.; Edwards, A. K.; Goodman, G. L.; Berkowitz, J. *J. Chem. Phys.* **1982**, *77*, 5508. Bruna, P. J.; Peyerimhoff, S. D.; Buenker, R. *J. Chem. Phys.* **1978**, *27*, 33.

(17) Gauld, J. W.; Radom, L. *J. Phys. Chem.* **1994**, *98*, 777.

(18) Nguyen, M. T.; Creve, S.; Vanquickenborne, L. G. *J. Phys. Chem.* **1996**, *100*, 18422.

(19) Lias, S. G.; Bartmess, J. E.; Liebman, J. F.; Holmes, J. L.; Levin, R. D.; Mallard, W. G. *J. Phys. Chem. Ref. Data, Suppl.* **1988**, 17.

(20) Schweighofer, A.; Chou, P. K.; Thoen, K. K.; Nanayakkara, V. K.; Keck, H.; Kuchen, W.; Kenttamaa, H. I. *J. Am. Chem. Soc.* **1996**, *118*, 11893. Chiu, S-W.; Li, W.-K.; Tzeng, W.-B.; Ng, C.-Y. *J. Chem. Phys.* **1992**, *97*, 6557. Nobes, R. H.; Bouma, W. J.; Radom, L. *J. Am. Chem. Soc.* **1984**, *106*, 2774. Yates, B. F.; Bouma, W. J.; Radom, L. *J. Am. Chem. Soc.* **1987**, *109*, 2250.

(21) Pope, S. A.; Hillier, I. H.; Guest, M. F. *Chem. Phys. Lett.* **1984**, *104*, 191.

(22) Nobes, R. H.; Radom, L. *Chem. Phys. Lett.* **1992**, *189*, 554.

(23) Curtiss, L. A.; Nobes, R. H.; Pople, J. A.; Radom, L. *J. Chem. Phys.* **1992**, *97*, 6766.

(24) Flores, J. R.; Barrientos, C.; Largo, A. *J. Phys. Chem.* **1994**, *98*, 1090.

(25) Pope, S. A.; Hillier, I. H.; Guest, M. F. *J. Am. Chem. Soc.* **1985**, *107*, 3789.

(26) Frisch, M. J.; Trucks, G. W.; Gordon, M. H.; Gill, P. M. W.; Wong, M. W.; Foresman, J. B.; Johnson, B. G.; Schlegel, H. B.; Robb, M. A.; Replogle, E. S.; Gomperts, R.; Andres, J. L.; Raghavachari, K.; Binkley, J. S.; Gonzalez, C.; Martin, R. J.; Fox, D. J.; Defrees, B. J.; Baker, J.; Stewart, J. J. P.; Pople, J. A. *Gaussian 94*; Gaussian Inc., Pittsburgh, PA, 1994.